Int. J. Heat Mass Transfer. Vol. 28, No. 3, pp. 683–697, 1985
Printed in Great Britain

0017–9310/85 $3.00 + 0.00

The Brinkman model for natural convection about a semi-infinite vertical flat plate in a porous medium

C. T. HSU

Fluid Mechanics Department, TRW Space and Technology Group, Redondo Beach, CA 90278, U.S.A.

and

P. CHENG

Department of Mechanical Engineering, University of Hawaii at Manoa, Honolulu, HI 96822, U.S.A.

(*Received* 19 *April* 1984 *and in final form* 3 *October* 1984)

Abstract—The Brinkman model is used for the theoretical study of boundary effects in a natural convection porous layer adjacent to a semi-infinite vertical plate with a power law variation of wall temperature, i.e. $\bar{T}_w \alpha \bar{x}^{\lambda}$. It is shown that the dimensionless governing equations based on this model contain two parameters $\varepsilon = (Ra)^{-1/2}$ and $\sigma = (Da/\phi)^{1/2}$ where Ra and Da are the Rayleigh number and the Darcy number based on a reference length and ϕ is the porosity. For the limit of $\varepsilon \to 0$, $\sigma \to 0$ and $\sigma \ll \varepsilon$, a perturbation solution for the problem is obtained based on the method of matched asymptotic expansions. The physical problem can then be visualized to be consisting of three layers: an inner viscous sublayer, adjacent to the heated surface, with a thickness of the order of $0(\sigma)$; a middle thermal layer of thickness of the order of $0(\varepsilon)$; and the outer potential flow region with thickness of the order of 0(1). It is found that the first-order problem of the thermal layer is identical to that based on Darcy's law with slip flow, whose solution was obtained previously. Composite solutions for stream function and temperature, uniformly valid everywhere in the flow field, are constructed from the solutions for the thermal layer and the viscous sublayer. A new parameter Pn_x, defined as $Pn_x = (Ra_x Da_x)^{1/2}$ with Ra_x and Da_x denoting the local Rayleigh number and the local Darcy number based on $\bar{x}$, is found to be a measure of the boundary effect. It is shown that the viscous effect on the boundary has a drastic effect on the streamwise velocity component near the wall with a lesser effect on heat transfer characteristics. The boundary effect slows down the buoyancy-induced flow with a resulting decrease in heat transfer. The local Nusselt number is found to be of the form $Nu_x/(Ra_x)^{1/2} = C_1 - C_2 Pn_x$ where the values of C_1 and C_2 depending on λ. For an isothermal vertical plate ($\lambda = 0$), the first-order correction to the local Nusselt number is identically zero, i.e. $C_2 = 0$. In general, the boundary effect on the local Nusselt number becomes more pronounced as the value of Pn_x, Ra_x or Da_x is increased.

1. INTRODUCTION

WITH a few exceptions, most of the published theoretical work on convective heat transfer use Darcy's law as the momentum equation [1]. It is well known that Darcy's law is an empirical formula relating the pressure gradient, the bulk viscous resistance and the gravitational force in a porous medium. Thus, the formulation of convective heat transfer problems based on Darcy's law completely neglects the viscous force acting along the impermeable surface. Mathematically, since the order of Darcy's law is lower than the Navier–Stokes equation, the no-slip boundary condition is not required to be imposed on the impermeable boundary. The inability to satisfy the no-slip boundary conditions has aroused some concerns in the past as to whether Darcy's law is indeed adequate for the formulation of convective heat transfer problems in porous media.

For flow through a porous medium with a high permeability, Brinkman [2] as well as Chan *et al.* [3] argue that the momentum equation for porous media flow must reduce to the viscous flow limit and advocate that classical frictional terms be added in Darcy's law. This *ad hoc* equation has since become known as the Brinkman model. It was derived more rigorously later by Tam [4] and Lundgren [5]. The Brinkman model was used by Chan *et al.* [3] to study convective heat transfer in an enclosed gas-filled porous medium. It was also used by Katto and Masuoka [6] as well as by Walker and Homsy [7] for the studies of onset of free convection of liquids in a porous medium bounded between parallel plates and heated from below. In particular, Walker and Homsy [7] found that the critical parameter for the onset of free convection depends on the Darcy number Da, defined as $Da = K/H^2$ where K is the permeability of the porous medium and H is the distance between the parallel plates. Based on the Brinkman model with no-slip boundary conditions imposed, Rudraiah and Masuoka [8] have studied convective heat transfer in a horizontal porous layer heated from below with a free surface at the top. With the assumption that convective terms in the energy equation are negligible, the resulting linear equations were solved analytically based on the method of matched asymptotic expansions. It is found that the no-slip boundary

NOMENCLATURE

A constant defined in equation (9c)
A_2 constant defined in equation (87)
B_0, B_1, B_2 constants given by equations (62), (73) and (91)
C_1, C_2 constants given by equation (132b)
D_0, D_1, D_2 constants given by equations (67), (85) and (104)
Da Darcy number based on l, $Da = K/l^2$
Da_x local Darcy number (K/x^2)
f_0, f_1, f_2 dimensionless perturbation stream functions in the thermal layer
g gravitational acceleration
g_0, g_1, g_2 dimensionless perturbation temperature functions in the thermal layer
H distance between two parallel plates
K permeability of the porous medium
k thermal conductivity of the saturated porous medium
L a reference dimensional length
l dimensional length of the plate
Nu_x local Nusselt number, $\bar{q}\bar{x}/k(\bar{T}_w - \bar{T}_\infty)$
$\overline{Nu}$ average Nusselt number, $\bar{Q}/k(\overline{T_w - T_\infty})$
p pressure
Pn_x local no-slip (boundary) parameter, $\sqrt{\dfrac{K^2\rho_\infty\beta g A X^{\lambda-1}}{\phi\mu\alpha L^{1-\lambda}}}$
Pn no-slip (boundary) parameter based on l, $\sqrt{\dfrac{K^2\rho_\infty\beta g A l^{2(\lambda-1)}}{\phi\mu\alpha}}$
$\bar{Q}$ total heat transfer rate
Ra_x local Rayleigh number, $\rho_\infty K\beta g(\bar{T}_w - \bar{T}_\infty)x/\mu\alpha$
Ra Rayleigh number based on L, $\rho_\infty K\beta g A L^{\lambda+1}/\mu\alpha$
$\bar{T}$ dimensional temperature
u dimensionless velocity in the x-direction
$\bar{u}$ dimensional velocity in the x-direction
v dimensionless velocity in the y-direction
$\bar{v}$ dimensional velocity in the y-direction
x dimensionless coordinate along the plate, $\bar{x}/L$
$\bar{x}$ dimensional coordinate along the plate
X dimensionless coordinate in the thermal layer, x
$\hat{X}$ dimensionless coordinate in the viscous sublayer, X
y dimensionless coordinate perpendicular to the plate, $\bar{y}/L$
$\bar{y}$ dimensional coordinate perpendicular to the plate
Y dimensionless coordinate in the thermal layer, y/ε
$\hat{Y}$ dimensionless coordinate in the viscous sublayer, Y/Γ.

Greek symbols

α equivalent thermal diffusivity
β thermal expansion coefficient of fluid
Γ perturbation parameter, σ/ε
ε perturbation parameter, $(Ra)^{-1/2}$
η similarity variable, $X^{(\lambda-1)/2}Y$
Θ dimensionless temperature in the thermal layer
θ dimensionless temperature, $(\bar{T} - \bar{T}_\infty)/AL^\lambda$
λ prescribed wall temperature parameter
μ viscosity of fluid
ρ density of fluid
σ dimensionless parameter, Da/ϕ
ϕ porosity
ψ dimensionless stream function, $\mu\bar{\psi}/\rho_\infty g K\beta A L^{\lambda+1}$
$\bar{\psi}$ dimensional stream function
Ψ dimensionless stream function in the thermal layer, ψ/ε.

Superscript

$^-$ dimensional quantities.

Subscript

∞ condition at infinity
w condition at the wall
c composite solution.

condition has important effects on the streamwise velocity near the impermeable surface but its effect on temperature distribution is negligible.

Using the volumetric averaging technique, Vafai and Tien [9] have extended the Brinkman model to include the inertia effect. The resulting equation was solved numerically for the problem of forced convection along a heated plate embedded in a porous medium. Vafai and Tien [9] defined a momentum boundary layer as the layer adjacent to the impermeable surface where the viscous effect on the surface and the bulk viscous force are equally important. The existence of the momentum boundary layer near the heated surface was shown to retard the streamwise velocity near the wall, resulting in

a decrease of the surface heat flux. The effect is found to be most pronounced near the leading edge and in a fluid with a high Prandtl number.

The Brinkman model with the addition of the convective terms and under the boundary-layer approximation was used by Evans and Plumb [10] for a numerical study of free convection about an isothermal vertical plate in a porous medium. Their numerical results show that the value of the local Nusselt number is in agreement with the Cheng–Minkowycz theory [11] (based on Darcy's law) if the Darcy number based on the length of the plate is less than 10^{-7}. For higher values of the Darcy number, they found that their numerical results for the local Nusselt number are slightly smaller than those given by the Cheng–Minkowycz theory [11].

In this paper, we shall re-examine Cheng and Minkowycz's problem based on the Brinkman model and the method of matched asymptotic expansions. It will be shown that the dimensionless governing equations contain two small dimensionless parameters ε and σ, where $\varepsilon = 1/(Ra)^{1/2}$ and $\sigma = (Da/\phi)^{1/2}$ with Ra and Da (defined later) as the Rayleigh number and the Darcy number respectively. The problem can then be considered to consist of three layers: the inner viscous sublayer with a thickness of $0(\sigma)$ which has been called the momentum boundary layer by Vafai and Tien [9]; the middle thermal layer with a thickness of $0(\varepsilon)$; and the outer potential region with a thickness of 0(1). For the case of $\sigma/\varepsilon \ll 1$, which is the case that usually exists in geophysical and engineering applications, the thickness of the viscous sublayer is smaller than that of the thermal layer. By the method of matched asymptotic expansions, it is shown that the governing equations for the thermal layer are identical to those using Darcy's law as the momentum equation, while those for the inner viscous sublayer are governed by another set of simplified equations with no-slip boundary conditions and thermal boundary conditions imposed. The solutions for the thermal layer and the viscous sublayer are then matched at the interface, thereby resulting in a uniformly valid solution. The eigenfunctions associated with the thermal layer are found to be identical to those given in a previous paper [12]. Since the constants associated with the eigenfunctions cannot be determined without a detailed analysis of the leading edge effect, the perturbation series for the thermal layer is truncated to the term which the leading edge effect begins to appear. A new boundary friction parameter Pn_x (where $Pn_x = [K^2\rho_\infty g(T_w - T_\infty)/\phi\mu\alpha x]^{1/2}$), defined as the local thickness ratio of the viscous sublayer and the thermal layer at $\bar{x}$, emerges in the present analysis as the governing parameter for the boundary friction effect. It is shown that this effect tends to decrease the heat transfer rate, and that it becomes more pronounced when the prescribed wall temperature deviates from that of the isothermal. Although the boundary friction has no effect on the local Nusselt number to the first-order approximation, its effect on the average Nusselt number depends on the value of P_n, the boundary friction parameter based on the length of the plate.

2. FORMULATION OF THE PROBLEM

Consider the problem of steady, two-dimensional free convection in a porous medium adjacent to a vertical semi-infinite plate. Under the assumptions that the porous medium is in local thermal equilibrium, the properties of the fluid and the porous matrix are constant and isotropic, and the Boussinesq approximation is applicable, the governing equations with inertia and thermal dispersion effects neglected are

$$\bar{u}_{\bar{x}} + \bar{u}_{\bar{y}} = 0 \tag{1}$$

$$\frac{\mu\bar{u}}{K} = \frac{\mu}{\phi}(\bar{u}_{\bar{x}\bar{x}} + \bar{u}_{\bar{y}\bar{y}}) - \bar{p}_{\bar{x}} - \bar{\rho}g \tag{2}$$

$$\frac{\mu\bar{v}}{K} = \frac{\mu}{\phi}(\bar{v}_{\bar{x}\bar{x}} + \bar{v}_{\bar{y}\bar{y}}) - \bar{p}_{\bar{y}} \tag{3}$$

$$\bar{\rho} = \rho_\infty[1 - \beta(\bar{T} - \bar{T}_\infty)] \tag{4}$$

$$\bar{u}\bar{T}_{\bar{x}} + \bar{v}\bar{T}_{\bar{y}} = \alpha(\bar{T}_{\bar{x}\bar{x}} + \bar{T}_{\bar{y}\bar{y}}) \tag{5}$$

where $\bar{x}$ is the coordinate placed on the vertical plate and $\bar{y}$ is the coordinate perpendicular to the plate and pointing toward the porous medium. $\bar{u}$ and $\bar{v}$ are the Darcy velocities in the $\bar{x}$- and y-directions; ρ_∞, β and μ are the density of the fluid at infinity, the thermal expansion coefficient of the fluid and the viscosity of the fluid; g is the gravitational acceleration; K is the permeability of the porous medium; ϕ is the porosity; α is the equivalent thermal diffusivity of the porous medium; and $\bar{T}$ is the temperature. It is relevant to mention that equations (2) and (3) are the Brinkman model for porous media flow.

Eliminating $\bar{p}$ between equations (2) and (3), and expressing the resulting equations in terms of the stream function $\bar{\psi}$ and temperature $\bar{T}$, yields

$$\bar{\psi}_{\bar{x}\bar{x}} + \bar{\psi}_{\bar{y}\bar{y}} = \frac{\rho_\infty\beta g K}{\mu}\bar{T}_{\bar{y}} + \frac{K}{\phi}(\bar{\psi}_{\bar{x}\bar{x}\bar{x}\bar{x}} + 2\bar{\psi}_{\bar{x}\bar{x}\bar{y}\bar{y}} + \bar{\psi}_{\bar{y}\bar{y}\bar{y}\bar{y}}) \tag{6}$$

$$\alpha(\bar{T}_{\bar{x}\bar{x}} + \bar{T}_{\bar{y}\bar{y}}) = \bar{T}_{\bar{x}}\bar{\psi}_{\bar{y}} - \bar{T}_{\bar{y}}\bar{\psi}_{\bar{x}} \tag{7}$$

where the stream function $\bar{\psi}$ satisfies

$$\bar{u} = \bar{\psi}_{\bar{y}} \quad \text{and} \quad \bar{v} = -\bar{\psi}_{\bar{x}}. \tag{8a,b}$$

If the temperature of the semi-infinite vertical surface is a power function of distance from the leading edge, the boundary conditions at the wall are

$$\bar{y} = 0,\ \bar{x} \geqslant 0:\ \bar{\psi} = \bar{\psi}_{\bar{y}} = 0, \quad \bar{T}_w = \bar{T}_\infty + A\bar{x}^\lambda \tag{9a,b,c}$$

$$\bar{y} = 0,\ \bar{x} < 0:\ \bar{\psi} = \bar{\psi}_{\bar{y}} = 0, \quad \bar{T}_w = \bar{T}_\infty. \tag{10a,b,c}$$

where equations (9b) and (10b) are the no-slip boundary conditions and $\bar{T}_\infty$ is the temperature at infinity. The boundary conditions at infinity are

$$\bar{y} \to \infty; \quad \bar{\psi}_{\bar{y}} = 0; \quad \bar{T} = \bar{T}_\infty. \tag{11a,b}$$

We now introduce the following dimensionless variables

$$\psi = \frac{\mu\bar{\psi}}{\rho_\infty g K\beta A L^{\lambda+1}}, \quad \theta = \frac{\bar{T}-\bar{T}_\infty}{AL^\lambda}, \quad x = \bar{x}/L, \quad y = \bar{y}/L \tag{12}$$

where L is a reference length. In terms of these dimensionless variables, equations (6) and (7) become

$$\psi_{xx}+\psi_{yy} = \theta_y+\sigma^2(\psi_{xxxx}+2\psi_{xxyy}+\psi_{yyyy}) \tag{13}$$

$$\varepsilon^2(\theta_{xx}+\theta_{yy}) = \theta_x\psi_y-\theta_y\psi_x \tag{14}$$

and boundary conditions (9)–(11) become

$$\psi(x,0)=0, \quad \psi_y(x,0)=0, \quad \theta(x,0)=x^\lambda, \quad x\geqslant 0 \tag{15a,b,c}$$

$$\psi(x,0)=0, \quad \psi_y(x,0)=0, \quad \theta(x,0)=0, \quad x<0 \tag{16a,b,c}$$

$$\psi_y(x,\infty)=0, \quad \theta(x,\infty)=0. \tag{17a,b}$$

In equations (13) and (14), $\varepsilon=(Ra)^{-1/2}$ and $\sigma=(Da/\phi)^{1/2}$ with $Ra=\rho_\infty K\beta gAL^{\lambda+1}/\mu\alpha$ and $Da=K/L^2$ where both ε and σ are small dimensionless parameters. For the case when $\sigma\ll\varepsilon$ or $\Gamma=\sigma/\varepsilon\ll 1$ which exists in most of the geophysical and engineering applications, the problem then consists of three layers with the innermost viscous sublayer of thickness $0(\sigma)$, the middle thermal layer of thickness $0(\varepsilon)$, and the outer flow region of thickness 0(1). Note that equation (13) states that the flow vorticity $\psi_{xx}+\psi_{yy}$ is generated by the thermal gradient θ_y and viscous shear $\sigma^2(\psi_{xxxx}+2\psi_{xxyy}+\psi_{yyyy})$. It follows that the outer region where thermal gradients and viscous shear vanish, is a potential flow region. Equations (13) and (14) become singular as $\varepsilon\to 0$ and $\sigma\to 0$ since the highest order terms in these equations vanish under these limits.

Governing equations for thermal boundary layer

To incorporate the thermal gradient effect, we stretch the horizontal scale based on the thermal boundary-layer thickness which is of $0(\varepsilon)$, i.e.

$$Y = y/\varepsilon \quad \text{and} \quad X = x. \tag{18}$$

The work of Cheng and Minkowycz [11] suggests that when $\theta=0(1)$ in the thermal boundary layer, ψ is of $0(\varepsilon)$. Thus, the dependent variables in the thermal boundary layer that are of 0(1) are

$$\Theta=\theta, \quad \Psi=\psi/\varepsilon. \tag{19}$$

In terms of these variables, equations (13) and (14) become

$$\varepsilon^2\Psi_{XX}+\Psi_{YY} = \Theta_Y+\Gamma^2[\varepsilon^4\Psi_{XXXX}+2\varepsilon^2\Psi_{XXYY}+\Psi_{YYYY}] \tag{20}$$

$$\varepsilon^2\Theta_{XX}+\Theta_{YY} = \Theta_X\Psi_Y-\Theta_Y\Psi_X \tag{21}$$

where $\Gamma=\sigma/\varepsilon=\sqrt{(K^2\rho_\infty\beta gA/\phi\mu\alpha L^{1-\lambda})}$ is the ratio of the viscous layer thickness to the thermal layer thickness. In equations (20) and (21), the first term with ε^2 represents the effect of outer inviscid flow on the thermal layer while terms with Γ represent the effect of viscous layer on the thermal layer. Thus, letting $\Gamma=0$ is equivalent to neglecting the viscous layer effect, as discussed by Cheng and Hsu [12] in a previous paper. In the present study, we shall neglect the effect of outer flow and consider only the interaction between the viscous layer and the thermal layer. For this reason, we let $\varepsilon=0$ in equations (20) and (21) which leads to

$$\Psi_{YY} = \Theta_Y+\Gamma^2\Psi_{YYYY} \tag{22}$$

$$\Theta_{YY} = \Theta_X\Psi_Y-\Theta_Y\Psi_X. \tag{23}$$

Equations (22) and (23) are the approximate equations for the thermal layer, which will be solved subject to the following boundary conditions

$$Y\to\infty, \quad \Psi_Y=\Theta=0 \tag{24}$$

$$Y\to 0: \ \Psi \text{ and } \Theta \text{ match with the solution for the viscous sublayer.} \tag{25}$$

Governing equations for the viscous sublayer

To examine the viscous effect near the heated surface, we shall stretch Y further by length scale Γ so that

$$\hat{X}=X \quad \text{and} \quad \hat{Y}=Y/\Gamma. \tag{26a,b}$$

In the viscous sublayer, we expect ψ is small, and θ remains to be of 0(1). Hence, the dependent variables in the viscous sublayer are

$$\hat{\Psi}=\psi/\sigma, \hat{\Theta}=\theta \text{ and therefore } \hat{\Psi}=\Psi/\Gamma. \tag{27a,b,c}$$

Equations (22) and (23) in terms of the viscous sublayer variables given by equations (26) and (27) are

$$\hat{\Psi}_{\hat{Y}\hat{Y}} = \hat{\Theta}_{\hat{Y}}+\hat{\Psi}_{\hat{Y}\hat{Y}\hat{Y}\hat{Y}} \tag{28}$$

$$\hat{\Theta}_{\hat{Y}\hat{Y}} = \Gamma^2[\hat{\Theta}_{\hat{X}}\hat{\Psi}_{\hat{Y}}-\hat{\Theta}_{\hat{Y}}\hat{\Psi}_{\hat{X}}]. \tag{29}$$

Equations (28) and (29) are the approximate equations for the viscous sublayer, which are to be solved subject to the following boundary conditions

$$\hat{\Psi}_{\hat{Y}}(\hat{X},0)=\hat{\Psi}(\hat{X},0)=0 \tag{30}$$

$$\hat{\Theta}(\hat{X},0)=\hat{X}^\lambda \tag{31}$$

and $\hat{\Psi}$ and $\hat{\Theta}$ must match with the solution for the thermal layer to the appropriate order.

3. SOLUTIONS BY MATCHED ASYMPTOTIC EXPANSIONS

For the thermal layer, the following series expansions will be made:

$$\Psi(X,Y;\Gamma) = \Psi_0(X,Y)+\Gamma\Psi_1(X,Y)+\Gamma^2\Psi_2(X,Y)+0(\Gamma^3) \tag{32}$$

$$\Theta(X,Y;\Gamma) = \Theta_0(X,Y)+\Gamma\Theta_1(X,Y)+\Gamma^2\Theta_2(X,Y)+0(\Gamma^3). \tag{33}$$

Substituting equations (32) and (33) into (22) and (23) yields the following first-order problem

$$\Psi_{0YY} = \Theta_{0Y} \tag{34}$$

$$\Theta_{0YY} = \Theta_{0X}\Psi_{0Y} - \Theta_{0Y}\Psi_{0X} \tag{35}$$

subject to the boundary conditions

$$\Psi_{0Y}(X, \infty) = \Theta_0(X, \infty) = 0 \tag{36a, b}$$

and Ψ_0 and Θ_0 must match with the solution for the viscous sublayer as $Y \to 0$.

The second-order problem for the thermal layer is

$$\Psi_{1YY} = \Theta_{1Y} \tag{37}$$

$$\Theta_{1YY} = \Theta_{1X}\Psi_{0Y} - \Theta_{0Y}\Psi_{1X} + \Theta_{0X}\Psi_{1Y} - \Theta_{1Y}\Psi_{0X} \tag{38}$$

subject to the boundary conditions

$$\Psi_{1Y}(X, \infty) = \Theta_1(X, \infty) = 0 \tag{39a,b}$$

and Ψ_1 and Θ_1 must match with the solution for the viscous sublayer as $Y \to 0$.

The third-order problem for the thermal layer is

$$\Psi_{2YY} = \Theta_{2Y} + \Psi_{0YYYY} \tag{40}$$

$$\Theta_{2YY} = \Theta_{0X}\Psi_{2Y}\Psi_{2Y} + \Theta_{2X}\Psi_{0Y} - (\Theta_{0Y}\Psi_{2X} + \Theta_{2Y}\Psi_{0X}) - (\Theta_{1Y}\Psi_{1X} - \Theta_{1X}\Psi_{1Y}) \tag{41}$$

subject to the boundary conditions

$$\Psi_{2Y}(X, \infty) = \Theta_2(X, \infty) = 0 \tag{42a,b}$$

and Ψ_2 and Θ_2 must match with the solution for the viscous sublayer as $Y \to 0$.

For the viscous sublayer, the following expansions will be made:

$$\hat{\Psi}(\hat{X}, \hat{Y}; \Gamma) = \hat{\Psi}_0(\hat{X}, \hat{Y}) + \Gamma\hat{\Psi}_1(\hat{X}, \hat{Y}) + \Gamma^2\hat{\Psi}_2(\hat{X}, \hat{Y}) + 0(\Gamma^3) \tag{43}$$

$$\hat{\Theta}(\hat{X}, \hat{Y}; \Gamma) = \hat{\Theta}_0(\hat{X}, \hat{Y}) + \Gamma\hat{\Theta}_1(\hat{X}, \hat{Y}) + \Gamma^2\hat{\Theta}_2(\hat{X}, \hat{Y}) + 0(\Gamma^3). \tag{44}$$

Substituting equations (43) and (44) into (28) and (29) and equating the different order in Γ yields the following linear sub-problems for the viscous sublayer.

The first-order problem for the viscous sublayer. The governing equations are

$$\hat{\Psi}_{0\hat{Y}\hat{Y}} = \hat{\Theta}_{0\hat{Y}} + \hat{\Psi}_{0\hat{Y}\hat{Y}\hat{Y}\hat{Y}} \tag{45}$$

$$\hat{\Theta}_{0YY} = 0 \tag{46}$$

subject to the boundary conditions

$$\hat{\Psi}_0(\hat{X}, 0) = \hat{\Psi}_{0\hat{Y}}(\hat{X}, 0) = 0, \quad \hat{\Theta}_0(\hat{X}, 0) = \hat{X}^\lambda \tag{47a,b,c}$$

and $\hat{\Psi}_0$ and $\hat{\Theta}_0$ must match with the solution for the thermal layer as $\hat{Y} \to \infty$.

The second-order problem for the viscous sublayer. The governing equations are

$$\hat{\Psi}_{1\hat{Y}\hat{Y}} = \hat{\Theta}_{1\hat{Y}} + \hat{\Psi}_{1\hat{Y}\hat{Y}\hat{Y}} \tag{48}$$

$$\hat{\Theta}_{1\hat{Y}\hat{Y}} = 0 \tag{49}$$

subject to the boundary conditions

$$\hat{\Psi}_1(\hat{X}, 0) = \hat{\Psi}_{1\hat{Y}}(\hat{X}, 0) = 0, \quad \hat{\Theta}_1(\hat{X}, 0) = 0 \tag{50a,b,c}$$

and $\hat{\Psi}_1$ and $\hat{\Theta}_1$ must match with the solution for the thermal layer as $\hat{Y} \to \infty$.

The third-order problem for the viscous sublayer. The governing equations are

$$\hat{\Psi}_{2\hat{Y}\hat{Y}} = \hat{\Theta}_{2\hat{Y}} + \hat{\Psi}_{2\hat{Y}\hat{Y}\hat{Y}\hat{Y}} \tag{51}$$

$$\hat{\Theta}_{2\hat{Y}\hat{Y}} = \hat{\Theta}_{0\hat{X}}\hat{\Psi}_{0\hat{Y}} - \hat{\Theta}_{0\hat{Y}}\hat{\Psi}_{0\hat{X}} \tag{52}$$

subject to the boundary conditions

$$\hat{\Psi}_2(\hat{X}, 0) = \hat{\Psi}_{2\hat{Y}}(\hat{X}, 0) = 0, \quad \hat{\Theta}_2(\hat{X}, 0) = 0 \tag{53a,b,c}$$

and $\hat{\Psi}_2$ and $\hat{\Theta}_2$ must match with the solution for the thermal layer as $\hat{Y} \to \infty$.

4. MATCHING PROCEDURES

We now obtain solutions to the thermal layer and the viscous sublayer by asymptotic matching procedures.

The first-order solution for the thermal layer

Equations (34) and (35) with boundary conditions (36) are identical to the boundary-layer approximation for free convection in a porous medium adjacent to a heated vertical semi-infinite plate based on the Darcy law as the momentum equation. It has been shown by Cheng and Minkowycz [11] that the problem admits a similarity solution of the form

$$\Psi_0(X, Y) = X^{(\lambda+1)/2} f_0(\eta) \tag{54a}$$

$$\Theta_0(X, Y) = X^\lambda g_0(\eta) \tag{54b}$$

$$\eta = X^{(\lambda-1)/2} Y \tag{54c}$$

where $f_0(\eta)$ and $g_0(\eta)$ satisfy

$$f_0'' = g_0' \tag{55a}$$

$$g_0'' = \lambda f_0' g_0 - \frac{\lambda+1}{2} f_0 g_0' \tag{55b}$$

subject to boundary conditions

$$f_0(0) = 0, \quad g_0(0) = 1 \tag{56a, b}$$

$$f_0'(\infty) = g_0(\infty) = 0. \tag{57a, b}$$

Equation (55a) with the boundary conditions (57a, b) can be integrated once to yield

$$f_0' = g_0. \tag{58}$$

It follows from equations (54a), (54c), (56b) and (58) that

$$\text{as } Y \to 0, \quad \Psi_0(X, Y) = X^\lambda Y \tag{59}$$

which is the matching condition for the solution for the viscous sublayer.

The first-order solution for the viscous sublayer

The solution to equation (46) subject to the boundary condition (47c) is

$$\hat{\Theta}_0 = \hat{X}^\lambda + B_0(\hat{X})\hat{Y}. \tag{60}$$

To determine $B_0(\hat{X})$, equation (60) is rewritten in terms of the thermal layer variables as

$$\Theta_0 = X^\lambda + B_0(X) Y/\Gamma. \tag{61}$$

Under the condition that $\hat{\Theta}_0$ will not be more singular

than Θ_0, it is required that

$$B_0(X) = 0 \tag{62}$$

which can also be obtained by matching (61) to (54b) as $\eta \to 0$. It follows from equations (60) and (62) that

$$\hat{\Theta}_0 = \hat{X}^\lambda. \tag{63}$$

Substituting equation (63) into (45) and solving the resulting equation subject to the boundary conditions (47a,b) yields

$$\hat{\Psi}_0 = D_0(\hat{X})[e^{-\hat{Y}} + \hat{Y} - 1] \tag{64}$$

To determine $D_0(\hat{X})$, equation (64) is now rewritten in terms of the thermal layer variables

$$\Psi_0 = D_0(X)[\Gamma e^{-Y/\Gamma} + Y - \Gamma] \tag{65}$$

which indicates that to the first order, the location where the stream function equal to zero is displaced to $Y = \Gamma$ or $y = \sigma = (Da/\phi)^{1/2}$. In other words the displacement thickness produced by the viscous effect is equal to $(Da/\phi)^{1/2}$ which is a constant and independent of x. Expanding equation (65) for $\Gamma \to 0$ gives

$$\Psi_0 = D_0(X)Y. \tag{66}$$

Matching equation (66) with (59) gives

$$D_0(X) = X^\lambda \tag{67}$$

The second-order solution for the viscous sublayer

The solution to equation (49) subject to the boundary condition (50c) is

$$\hat{\Theta}_1(\hat{X}, \hat{Y}) = B_1(\hat{X})\hat{Y}. \tag{68}$$

From equations (44), (61), (62) and (68) the two-term expansion of $\hat{\Theta}$ for the viscous sublayer is

$$\hat{\Theta} = \hat{\Theta}_0(\hat{X}, \hat{Y}) + \Gamma\hat{\Theta}_1(\hat{X}, \hat{Y})$$
$$= \hat{X}^\lambda + \Gamma[B_1(\hat{X})\hat{Y}] + 0(\Gamma^2). \tag{69}$$

Rewriting the above equation in terms of the thermal layer variables yields

$$\Theta = X^\lambda + B_1(X)Y \quad \text{as } \hat{Y} \to \infty. \tag{70}$$

On the other hand, the one-term solution of Θ for the thermal layer as given by equations (31b) and (54c) is

$$\Theta = \Theta_0 = X^\lambda g_0(\eta). \tag{71}$$

Rewriting the above equation in the viscous sublayer variables and expanding for $\Gamma \to 0$ gives

$$\Theta = \hat{X}^\lambda + \hat{X}^{(3\lambda-1)/2} g_0'(0)\Gamma\hat{Y} \quad \text{as} \quad Y \to 0. \tag{72}$$

Matching equation (72) with (70) gives

$$B_1(\hat{X}) = \hat{X}^{(3\lambda-1)/2} g_0'(0). \tag{73}$$

Substituting equations (68) and (73) into (48) and solving the resulting equation subject to the boundary conditions (50a,b) yields

$$\hat{\Psi}_1(\hat{X}, \hat{Y}) = D_1(\hat{X})[e^{-\hat{Y}} + \hat{Y} - 1] + X^{(3\lambda-1)/2} \frac{g_0'(0)}{2} \hat{Y}^2 \tag{74}$$

where $D_1(\hat{X})$ remains to be determined.

From equations (43), (65), (67) and (74), the two-term solution of $\hat{\Psi}$ for the viscous sublayer is

$$\hat{\Psi} = \hat{\Psi}_0 + \Gamma\hat{\Psi}_1$$
$$= \hat{X}^\lambda[e^{-\hat{Y}} + \hat{Y} - 1] + \Gamma D_1(X)[e^{-\hat{Y}} + \hat{Y} - 1]$$
$$+ \frac{\Gamma}{2} g_0'(0)\hat{X}^{(3\lambda-1)/2}\hat{Y}^2 + 0(\Gamma^2). \tag{75}$$

Rewriting the above equation in terms of the thermal layer variables and expanding for $\Gamma \to 0$ gives

$$\Psi = \left[X^\lambda Y + \frac{g_0'(0)}{2} X^{(3\lambda-1)/2} Y^2\right]$$
$$+ \Gamma[-X^\lambda + D_1(X)Y] + 0(\Gamma^2). \tag{76}$$

The second-order solution for the thermal layer

Equations (37) and (38) are to be solved subject to the boundary conditions (39) and the matching conditions

$$\Psi_1(X, 0) = -X^\lambda \tag{77a}$$

$$\Theta_1(X, 0) = 0 \tag{77b}$$

where equation (77a) is obtained from equation (76) as $Y \to 0$ while equation (77b) is obtained from equation (70). It can be shown that equations (37) and (38) subject to the boundary conditions (39) and the matching conditions (77) admit a similarity solution of the form

$$\Psi_1(X, Y) = -X^\lambda f_1(\eta) \tag{78a}$$

$$\Theta_1(X, Y) = -X^{(3\lambda-1)/2} g_1(\eta) \tag{78b}$$

where $f_1(\eta)$ and $g_1(\eta)$ are determined from

$$f_1'' = g_1' \tag{79}$$

$$g_1'' = \frac{3\lambda - 1}{2} g_1 f_0' + \lambda g_0 f_1' - \frac{\lambda + 1}{2} f_0 g_1' - \lambda g_0' f_1 \tag{80}$$

subject to the boundary conditions

$$f_1(0) = 1, \quad g_1(0) = 0 \tag{81a,b}$$

$$f_1'(\infty) = g_1(\infty) = 0. \tag{82a,b}$$

For the special case of $\lambda = 0$, equations (79)–(82) give $g_1 = 0$ and $f_1 = 1$. Consequently, $\Psi_1 = -X^\lambda$ and $\Theta_1 = 0$, i.e. second-order corrections in temperature for the thermal layer are zero.

To determine $D_1(X)$ in equation (74), equation (78a) will be rewritten in terms of the viscous sublayer variables and then expanded for small Γ to give

$$\Psi_1(X, Y) = -X^\lambda - X^{(3\lambda-1)/2} f_1'(0)Y + \ldots. \tag{83}$$

where equation (81a) has been used. Thus, the two-term

expansion for Ψ in the thermal layer, as $\Gamma \to 0$ is

$$\Psi = X^{\lambda} Y + \frac{g_0'(0)}{2} X^{(3\lambda-1)/2} Y^2 - \Gamma[X^{\lambda} + X^{(3\lambda-1)/2} f_1'(0) Y + \ldots] + 0(\Gamma^2). \quad (84)$$

Matching equations (84) and (76) leads to

$$D_1(X) = -X^{(3\lambda-1)/2} f_1'(0) = 0 \quad (85)$$

since $f_1'(0) = 0$ which can be obtained by integrating equation (79) with the aid of equation (81b).

The third-order solution for the viscous sublayer

Substituting equations (63) and (66) into (52) and solving the resulting equation gives

$$\hat{\Theta}_2(\hat{X}, \hat{Y}) = A_2(\hat{X}) + B_2(\hat{X})\hat{Y} + \lambda \hat{X}^{2\lambda-1}[\hat{Y}^2/2 - e^{-\hat{Y}}]. \quad (86)$$

Imposing the boundary condition (53c) yields

$$A_2(\hat{X}) = \lambda \hat{X}^{2\lambda-1}. \quad (87)$$

To determine the function $B_2(X)$ in equation (86), the three-terms solution for the viscous sublayer will now be rewritten in terms of the thermal layer variables as

$$\Theta = \hat{\Theta}_0 + \Gamma\hat{\Theta}_1 + \Gamma^2\hat{\Theta}_2 = \left[X^{\lambda} + X^{(3\lambda-1)/2} g_0'(0) Y + \frac{\lambda X^{2\lambda-1}}{2} Y\right] + \Gamma B_2(X) Y + \Gamma^2 \lambda X^{2\lambda-1} + 0(\Gamma^3). \quad (88)$$

On the other hand, the two-term solution of Θ for the thermal layer is

$$\Theta = \Theta_0 + \Gamma\Theta_1 = X^{\lambda} g_0(\eta) - \Gamma X^{(3\lambda-1)/2} g_1(\eta) + 0(\Gamma^2). \quad (89)$$

Rewriting the above expression in terms of the viscous sublayer variables and expanding for small Γ yields

$$\Theta = X^{\lambda} + X^{(3\lambda-1)/2} g_0'(0) Y + \tfrac{1}{2} X^{2\lambda-1} g_0''(0) Y^2 - \Gamma[X^{2\lambda-1} g_1'(0) Y) + 0(\Gamma^2). \quad (90)$$

Matching equations (88) and (90) gives

$$B_2(X) = -X^{2\lambda-1} g_1'(0) \quad (91)$$

$$g_0''(0) = \lambda. \quad (92)$$

It is relevant to note that equation (92) could have been obtained from equation (55b) with the aid of equations (56a, b). Substituting equations (87) and (91) into (86) leads to

$$\hat{\Theta}_2(\hat{X}, \hat{Y}) = \lambda \hat{X}^{2\lambda-1}\left[1 + \frac{\hat{Y}^2}{2} - e^{-\hat{Y}}\right] - \hat{X}^{2\lambda-1} g_1'(0)\hat{Y}. \quad (93)$$

To determine $\hat{\Psi}_2$, equations (86) and (87) will now be substituted into equation (51). The resulting equation subject to the boundary conditions (53a, b) has the following solution

$$\hat{\Psi}_2(\hat{X}, \hat{Y}) = D_2(\hat{X})[e^{-\hat{Y}} + \hat{Y} - 1] + B_2(\hat{X})\hat{Y}^2/2 + \lambda \frac{\hat{X}^{2\lambda-1}}{6} \hat{Y}^3 \quad (94)$$

where $B_2(\hat{X})$ is given by equation (91) and $D_2(\hat{X})$ remains to be determined. It follows from equations (64), (67), (85), (74), (91) and (94) that the three-term solution of Ψ for the viscous sublayer is

$$\Psi = \Gamma\hat{\Psi}_0 + \Gamma^2\hat{\Psi}_1 + \Gamma^3\hat{\Psi}_2 + 0(\Gamma^4) = \Gamma\hat{X}^{\lambda}[e^{-\hat{Y}} + \hat{Y} - 1] + \Gamma^2\left[\frac{g_0'(0)}{2} \times \hat{X}^{(3\lambda-1)/2}\hat{Y}^2\right] + \Gamma^3\left\{D_2(\hat{X})[e^{-\hat{Y}} + \hat{Y} - 1] - \frac{g_1'(0)}{2}\hat{X}^{2\lambda-1}\hat{Y}^2 + \frac{\lambda}{6}\hat{X}^{2\lambda-1}\hat{Y}^3\right\} + 0(\Gamma^4). \quad (95)$$

Rewriting the above equation in terms of the thermal layer variables and expanding for small Γ gives

$$\Psi = X^{\lambda}\left[Y + \frac{g_0'(0)}{2} X^{(3\lambda-1)/2} Y^2 + \frac{\lambda}{6} X^{2\lambda-1} Y^3\right] - \Gamma\left[X^{\lambda} + \frac{g_1'(0)}{2} X^{2\lambda-1} Y^2\right] + \Gamma^2 D_2(X) Y. \quad (96)$$

The third-order solution for the thermal boundary layer

The matching conditions of the third-order equations for the thermal layer can be obtained from equations (93) and (96) which give

$$\Theta_2(X, 0) = \lambda X^{2\lambda-1} \quad (97a)$$

$$\Psi_2(X, 0) = 0. \quad (97b)$$

Substituting equations (54) and (78) into (40) and (41), it can be shown that the resulting equations, subject to the boundary conditions (42) and the matching conditions (97), admit a similarity solution of the form

$$\Psi_2(X, Y) = X^{(3\lambda-1)/2} f_2(\eta) \quad (98a)$$

$$\Theta_2(X, Y) = X^{2\lambda-1} g_2(\eta) \quad (98b)$$

where $f_2(\eta)$ and $g_2(\eta)$ are determined from

$$f_2'' = g_2' + f_0^{iv} \quad (99)$$

$$g_2'' = \lambda g_0 f_2' + (2\lambda - 1) g_2 f_0' - \frac{3\lambda - 1}{2} f_2 g_0' - \frac{\lambda + 1}{2} f_0 g_2' + \frac{3\lambda - 1}{2} g_1 f_1' - \lambda f_1 g_1' \quad (100)$$

subject to the boundary conditions

$$f_2(0) = 0, \quad g_2(0) = \lambda \quad (101a,b)$$

$$f_2'(\infty) = g_2(\infty) = 0. \quad (102a,b)$$

Rewriting equation (98a) in terms of the viscous

sublayer variables and expanding for small Γ gives

$$\Psi_2 = \Gamma X^{2\lambda-1} f_2(0) + Y X^{2\lambda-1} f_2'(0) = Y X^{2\lambda-1} f_2'(0) \quad (103)$$

where equation (101a) has been used. Matching equations (96) and (103) yields

$$D_2(X) = X^{2\lambda-1} f_2'(0) = 2\lambda X^{2\lambda-1} \quad (104)$$

where equation (99) has been used.

5. THE EIGENVALUE PROBLEM

The possible existence of the eigenfunctions associated with the higher-order problems for the thermal layer will now be investigated. Note that the homogeneous parts of the higher-order equations for the thermal layer as given by equations (37), (38), (40) and (41) are of the form

$$\Psi_{mYY} = \Theta_{mY} \quad (105)$$

$$\Theta_{mYY} = (\Theta_{0X}\Psi_{mY} + \Theta_{mX}\Psi_{0Y}) - (\Theta_{0Y}\Psi_{mX} + \Theta_{mY}\Psi_{0X}), \quad (106)$$

subject to the homogeneous boundary conditions

$$\Theta_m(X,0) = \Psi_m(X,0) = 0 \quad (107a,b)$$

$$\Theta_m(X,\infty) = \Psi_m(X,\infty) = 0. \quad (108a,b)$$

With the exception of the boundary condition (108b), equations (105)–(108a) are identical to the eigenvalue problem considered by Cheng and Hsu [12]. Following the procedures given in that paper, it can be shown that the eigensolutions are of the form

$$\Psi_m = X^{(\lambda+1)/2 + [(\lambda-1)/2]\beta_m} f_m(\eta) \quad (109a)$$

$$\Theta_m = X^{\lambda + [(\lambda-1)/2]\beta_m} g_m(\eta) \quad (109b)$$

where η is given by equation (54c). Substituting equations (109a,b) into (105)–(108) leads to

$$f_m'' = g_m' \quad (110)$$

$$g_m'' = \lambda g_0 f_m' + \left(\lambda + \frac{\lambda-1}{2}\beta_m\right) g_m f_0' - \left[\frac{\lambda+1}{2} + \left(\frac{\lambda-1}{2}\right)\beta_m\right] f_m g_0' - \frac{\lambda+1}{2} f_0 g_m' \quad (111)$$

subject to the boundary conditions

$$f_m(0) = g_m(0) = 0 \quad (112a,b)$$

$$f_m(\infty) = g_m(\infty) = 0. \quad (113a,b)$$

As in the previous paper [12], it will now be shown that Ψ_{0X} and Θ_{0X} are the eigenfunctions for the problem for $\lambda = 0$, i.e.

$$\Psi_m = \Psi_{0X} = X^{(\lambda-1)/2}\left[\frac{\lambda+1}{2} f_0 + \frac{\lambda-1}{2}\eta f_0'\right] \quad (114a)$$

$$\Theta_m = \Theta_{0X} = X^{\lambda-1}\left[\lambda g_0 + \frac{\lambda-1}{2}\eta g_0'\right]. \quad (114b)$$

To show that equations (114a,b) are indeed the eigenfunctions for $\lambda = 0$, equations (114a,b) are substituted into (105)–(108). It is found that equations (114a,b) satisfy (105) and (106) unconditionally, and that they satisfy boundary conditions (107) and (108) only if $\lambda = 0$. A comparison of equation (114a,b) and (109) for $\lambda = 0$ leads to

$$\beta_m = 2 \quad (115a)$$

$$f_m = (f_0 - \eta f_0')/2 \quad (115b)$$

$$g_m = -\eta g_0'/2. \quad (115c)$$

Equations (115b,c) are identical to the eigenfunctions obtained in the previous paper [12]. A comparison of equations (108a,b) and (66) and (67) of the previous paper [12] shows that

$$(\lambda-1)\beta_m = -(\lambda+1)\alpha_m \quad (116)$$

where α_ms are the eigenvalues in the previous paper [12]. Under the condition of equation (116), equations (110) and (111) are identical to (68) and (69) of the previous paper. Since α_m as a function of λ has already been computed [12], β_m can easily be determined as a function of λ according to equation (116). The results of these computations are listed in Table 1 which shows that $\alpha_m = \beta_m = 2$ for $\lambda = 0$ and $\beta_m > 2$ for $\lambda > 0$. As in the previous paper [12], the multiplicative constants associated with the eigenfunctions cannot be determined without a detailed analysis of the leading edge effect which is beyond the scope of this work. For this reason, the perturbation series is truncated to the term where leading edge effects begin to appear. It follows that for the thermal layer

(i) $\lambda = 0$:

$$\Psi = \Psi_0 + \Gamma\Psi_1 + 0(\Gamma^2 \log \Gamma) \quad (117a)$$

$$\Theta = \Theta_0 + 0(\Gamma^2 \log \Gamma) \quad (117b)$$

(ii) $\lambda > 0$:

$$\Psi = \Psi_0 + \Gamma\Psi_1 + \Gamma^2\Psi_2 + 0(\Gamma^3) \quad (118a)$$

$$\Theta = \Theta_0 + \Gamma\Theta_1 + \Gamma^2\Theta_2 + 0(\Gamma^3). \quad (118b)$$

It is relevant to note that the truncated terms for $\lambda = 0$ is of $0(\Gamma^2 \log \Gamma)$ since the eigenfunction for this case is of the order of Γ^2, which is of the same order as the next term in the postulated expansion [13]. Substituting the first, second and third-order solutions for the thermal

Table 1. Eigenvalues

λ	$-1/3$	0	0.1	1/3	1/2	3/4
α_m*	1.0	2.0	2.181	2.500	2.666	2.857
β_m	0.5	2.0	2.62	5.0	8.0	19.83

* Values taken from Cheng and Hsu [12].

layer in equations (117)–(118) gives

$$\Psi = \psi/\varepsilon = \begin{cases} X^{(\lambda+1)/2} f_0(\eta) - \Gamma X^{\lambda} + 0(\Gamma^2 \log \Gamma), & \lambda = 0 \quad (119a) \\ X^{(\lambda+1)/2} f_0(\eta) - \Gamma X^{\lambda} f_1(\eta) + \Gamma^2 X^{(3\lambda-1)/2} f_2(\eta) + 0(\Gamma^3), & \lambda > 0 \quad (119b) \end{cases}$$

$$\Theta = \theta = \begin{cases} X^{\lambda} g_0(\eta) + 0(\Gamma^2 \log \Gamma), & \lambda = 0 \quad (120a) \\ X^{\lambda} g_0(\eta) - \Gamma X^{(3\lambda-1)/2} g_1(\eta) + \Gamma^2 X^{2\lambda-1} g_2(\eta) + 0(\Gamma^3) & \lambda > 0. \quad (120b) \end{cases}$$

Similarly, if the perturbation series for the viscous sublayer is truncated to the same order, the stream function and temperature are given by

$$\hat{\psi} = \psi/\sigma = \begin{cases} \hat{X}^{\lambda}[e^{-\hat{Y}} + \hat{Y} - 1] + \Gamma \dfrac{g_0'(0)}{2} \hat{X}^{(3\lambda-1)/2} \hat{Y}^2 + \ldots, & \lambda = 0 \quad (121a) \\ \hat{X}^{\lambda}[e^{-\hat{Y}} + \hat{Y} - 1] + \Gamma \dfrac{g_0'(0)}{2} \hat{X}^{(3\lambda-1)/2} \hat{Y}^2 + \Gamma^2 \{2\lambda \hat{X}^{2\lambda-1}(e^{-\hat{Y}} + \hat{Y} - 1) \\ \qquad - \dfrac{g_1'(0)}{2} \hat{X}^{2\lambda-1} \hat{Y}^2 + \dfrac{\lambda}{6} \hat{X}^{2\lambda-1} \hat{Y}^3 \} + \ldots, & \lambda > 0 \quad (121b) \end{cases}$$

$$\hat{\Theta} = \theta = \begin{cases} \hat{X}^{\lambda} + \Gamma \hat{X}^{(3\lambda-1)/2} g_0'(0) \hat{Y} + \ldots, & \lambda = 0 \quad (122a) \\ \hat{X}^{\lambda} + \Gamma \hat{X}^{(3\lambda-1)/2} g_0'(0) \hat{Y} + \Gamma^2 \{\lambda \hat{X}^{2\lambda-1} - \hat{X}^{2\lambda-1} g_1'(0) \hat{Y} + \lambda \hat{X}^{2\lambda-1}[\hat{Y}^2/2 - e^{-\hat{Y}}]\} + \ldots, & \lambda > 0. \quad (122b) \end{cases}$$

6. RESULTS AND DISCUSSION

Higher-order solutions for the thermal layer

Higher-order solutions for the viscous sublayer are in terms of the algebraic and exponential functions which can easily be computed. However, higher-order solutions for the thermal layer are in the form of ordinary differential equations with two-point boundary conditions that must be integrated numerically. The numerical solutions of these higher-order equations for selected values of λ were carried out by the Runge–Kutta method with shooting procedures. The missing values of $g_0'(0)$, $g_1'(0)$ and $g_2'(0)$ as determined by this method for selected values of λ are listed in Table 2 for future reference.

Figure 1 shows that the value of f_1 are positive for all η. The variations of $f_1'(\eta)$ and $g_1(\eta)$ as a function of η are presented in Fig. 2 which shows that both of these quantities are negative. Because of the negative signs in front of these quantities in equations (78a,b), higher-order corrections to both the vertical velocity and temperature are positive for the thermal layer. The variation of $g_1'(\eta)$ is presented in Fig. 3 where it is shown that g_1' is negative at the wall and at small values of η; its value becomes positive at some intermediate value of η and approaches zero asymptotically at large η. For the case of $\lambda = 0$, $f_1' = g_1 = 0$ and $f_1 = 1$ which are shown as straight lines in Figs. 1–3. The second-order functions $f_2(\eta)$, $g_2(\eta)$ and $g_2'(\eta)$ are presented in Figs. 4–7, where it is shown that f_2 is always positive while the signs of g_2 and g_2' depend on the value of η.

Uniformly valid solutions

Uniformly valid solutions for stream function and temperature can be constructed by adding the inner and outer solutions and subtracting the common terms (i.e. the matching terms). For this purpose, equations (121a,b) for the viscous sublayer (i.e. the inner solution) are now rewritten in terms of the thermal variables to give

$$[\psi/\varepsilon]_{\text{inner}} = \begin{cases} X^{\lambda}[\Gamma e^{-Y/\Gamma} + Y - \Gamma] + \dfrac{g_0'(0)}{2} X^{(3\lambda-1)/2} Y^2 + 0(\Gamma^2 \log \Gamma) & \lambda = 0 \quad (123a) \\ X^{\lambda}[\Gamma e^{-Y/\Gamma} + Y - \Gamma] + \dfrac{g_0'(0)}{2} X^{(3\lambda-1)/2} Y^2 + 2\lambda X^{2\lambda-1}[\Gamma^3 e^{-Y/\Gamma} + \Gamma^2 Y - \Gamma^3] \\ \qquad - \Gamma \dfrac{g_1'(0)}{2} X^{2\lambda-1} Y^2 + \dfrac{\lambda}{6} X^{2\lambda-1} Y^3 + 0(\Gamma^4), & \lambda > 0 \quad (123b) \end{cases}$$

$$[\theta]_{\text{inner}} = \begin{cases} X^{\lambda} + X^{(3\lambda-1)/2} g_0'(0) Y + 0(\Gamma^2 \log \Gamma), & \lambda = 0 \quad (124a) \\ X^{\lambda} + X^{(3\lambda-1)/2} g_0'(0) Y + \Gamma^2 \lambda X^{2\lambda-1} - \Gamma X^{2\lambda-1} g_0'(0) Y \\ \qquad + \lambda X^{2\lambda-1}[Y^2/2 - \Gamma^2 e^{-Y/\Gamma}] + 0(\Gamma^3), & \lambda > 0. \quad (124b) \end{cases}$$

Table 2. Values of $g_0'(0)$, $g_1'(0)$ and $g_2'(0)$

	$\lambda = 0$	$\lambda = 0.1$	$\lambda = 1/3$	$\lambda = 1/2$	$\lambda = 3/4$
$g_0'(0)$*	−0.4437	−0.5235	−0.6776	−0.7703	−0.8923
$g_1'(0)$	0	−0.07897	−0.2049	−0.2822	−0.3926
$g_2'(0)$	†	0.2036	0.2613	−0.6406	−1.323

* Values taken from Cheng and Hsu [12].
† Value cannot be determined without a detailed analysis of the leading edge effect.

To obtain the matching terms, the above equations are expanded for $\Gamma \to 0$ (i.e. $\hat{Y} \to \infty$)

$$[\psi/\varepsilon]_{\text{matching}} = \begin{cases} X^{\lambda}[Y-\Gamma] + \dfrac{g_0'(0)}{2} X^{(3\lambda-1)/2} Y^2 + 0(\Gamma^2 \log \Gamma), & \lambda = 0 \quad (125a) \\ X^{\lambda}[Y-\Gamma] + \dfrac{g_0'(0)}{2} X^{(3\lambda-1)/2} Y^2 + 2\lambda X^{2\lambda-1}[\Gamma^2 Y - \Gamma^3] - \Gamma \dfrac{g_1'(0)}{2} X^{2\lambda-1} Y^2 & \\ \qquad + \dfrac{\lambda}{6} X^{2\lambda-1} Y^3 + 0(\Gamma^4), & \lambda > 0 \quad (125b) \end{cases}$$

$$[\theta]_{\text{matching}} = \begin{cases} X^{\lambda} + X^{(3\lambda-1)/2} g_0'(0) Y + 0(\Gamma^2 \log \Gamma), & \lambda = 0 \quad (126a) \\ X^{\lambda} + X^{(3\lambda-1)/2} g_0'(0) Y + \{\Gamma^2 \lambda X^{2\lambda-1} - \Gamma X^{2\lambda-1} g_0'(0) Y + \dfrac{\lambda}{2} X^{2\lambda-1} Y^2\}, & \lambda > 0. \quad (126b) \end{cases}$$

Thus, a composite solution (which is uniformly valid) for stream function can be obtained by adding equations (119a,b) to equations (123a,b) and subtracting equations (125a,b) to give

$$\lambda = 0: \Psi_c = X^{(\lambda+1)/2}\{f_0(\eta) - Pn_x[1 - e^{-\eta/Pn_x}]\} + 0(Pn_x^2 \log Pn_x) \quad (127a)$$

$$\lambda > 0: \Psi_c = X^{(\lambda+1)/2}\{f_0(\eta) - Pn_x[f_1(\eta) - e^{-\eta/Pn_x}] + Pn_x^2 f_2(\eta) + 2\lambda\, Pn_x^3 e^{-\eta/Pn_x}\} + 0(P_n^4) \quad (127b)$$

where Pn_x is the no-slip parameter defined as

$$Pn_x = \Gamma x^{(\lambda-1)/2} = \sqrt{(K^2 \rho_\infty \beta g A/\phi\mu\alpha L^{1-\lambda})}\, X^{(\lambda-1)/2} = \sqrt{Da_x Ra_x}$$

with $Da_x \equiv K/X^2$ and $Ra_x = \rho_\infty K\beta g A x^{\lambda+1}/\mu\alpha$ denoting the local Darcy number and the local Rayleigh number. It follows that a composite solution for the vertical velocity can be obtained by differentiating equations (127a,b) with respect to y to give

$$\lambda = 0: \frac{\mu \bar{u}_c}{\rho_\infty g\beta K(\bar{T}_w - \bar{T}_\infty)} = [f_0'(\eta) - e^{-\eta/Pn_x}] + 0(Pn_x^2 \log Pn_x) \quad (128a)$$

$$\lambda > 0: \frac{\mu \bar{u}_c}{\rho_\infty g\beta K(\bar{T}_w - \bar{T}_\infty)} = [f_0'(\eta) - e^{-\eta/Pn_x}] - Pn_x f_1'(\eta) + Pn_x^2[f_2'(\eta) - 2\lambda\, e^{-\eta/Pn_x}] + 0(Pr_x^3). \quad (128b)$$

Equation (128b) for $\lambda = 0.5$ and $Pn_x = 0.3$ is presented in Fig. 8, where it is shown that higher-order corrections to the vertical velocity are positive.

Similarly, a composite solution for temperature can be obtained by adding equations (120a,b) to (123a,b)

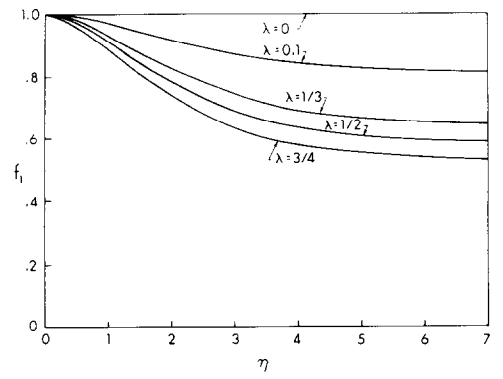

FIG. 1. f_1 vs η.

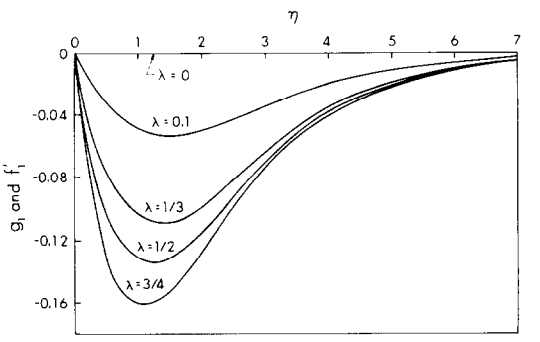

FIG. 2. g_1 and f_1' vs η.

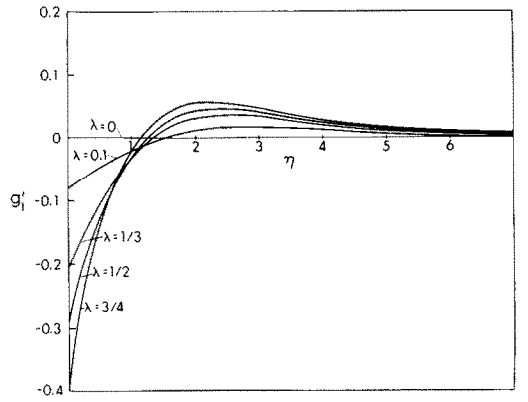

FIG. 3. g_1' vs η.

and subtracting the matching terms given by equations (126a,b) to give

$$\lambda = 0: \Theta_c = X^{\lambda} g_0(\eta) + 0(Pn_x^2 \log Pn_x) \quad (129a)$$

$$\lambda > 0: \Theta_c = X^{\lambda}\{g_0(\eta) - Pn_x g_1(\eta) + Pn_x^2[g_2(\eta) - \lambda e^{-\eta/Pn_x}]\} + 0(Pn_x^3). \quad (129b)$$

Equation (129b) for $\lambda = 0.5$ is shown in Fig. 9 where it is seen that the higher-order corrections to the temperature profile are also positive.

To illustrate the effects of the no-slip parameter Pn_x on the vertical velocity profile and temperature, equations (128b) and (129b) are plotted in Figs. 9 and 10 for $\lambda = 0.5$. The solid lines in these figures are the solutions based on Darcy's law [11] where the viscous effect on the impermeable surface is neglected. This corresponds to $Pn_x = 0$ in the present work. Figure 9 shows that the slip flow exists for the solution based on Darcy's law. As the no-slip parameter increases from zero, the maximum vertical velocity in the viscous sublayer begins to decrease from that of the slip velocity predicted by Darcy's law. The location at which the maximum buoyancy-induced velocity occurs is shown to increase from $\eta = 0$ (at the wall) to a finite distance

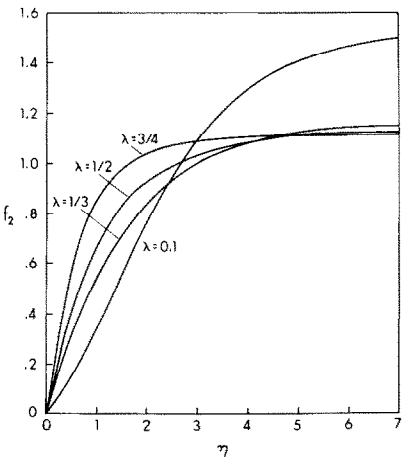

FIG. 4. f_2 vs η.

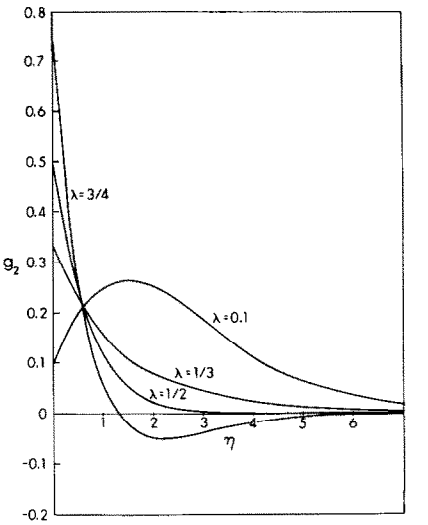

FIG. 5. g_2 vs η.

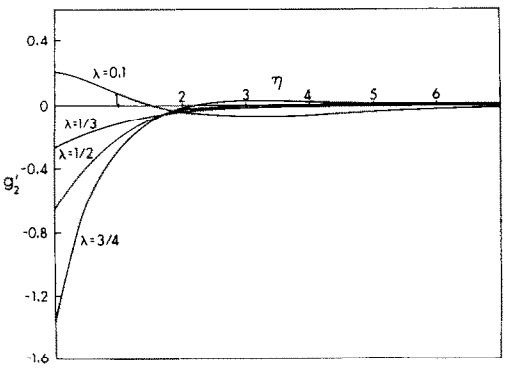

FIG. 6. g_2' vs η.

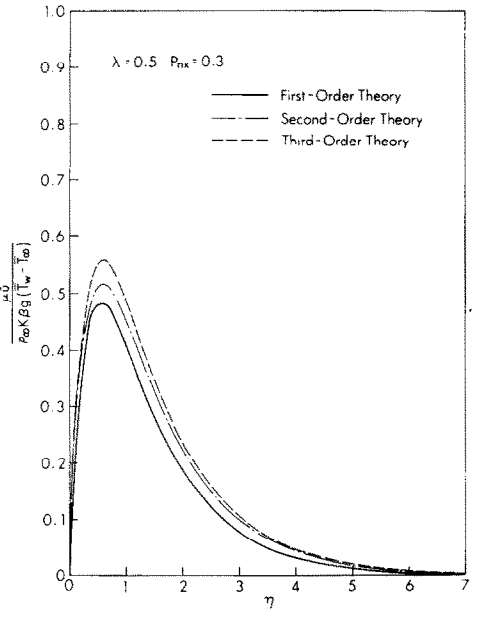

FIG. 7. Higher-order theory for velocity parallel to the heated plate.

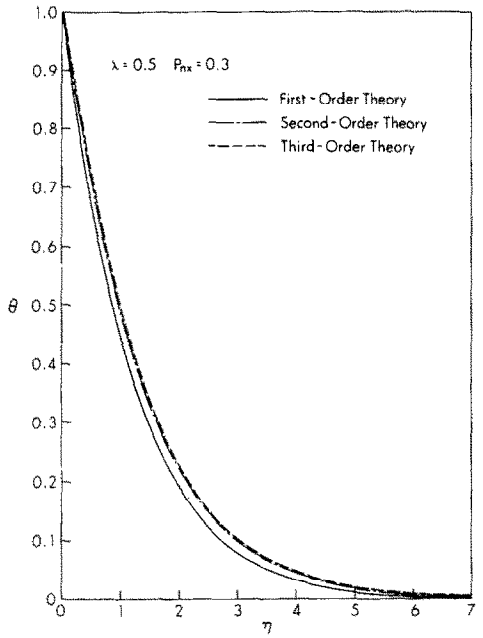

FIG. 8. Higher-order theory for temperature profiles.

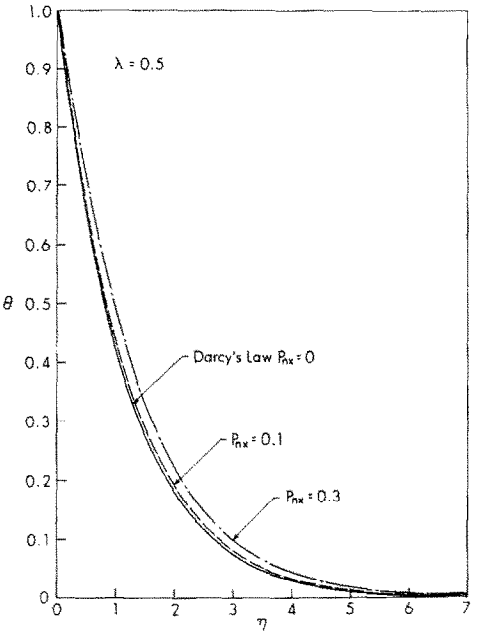

FIG. 10. Boundary effects on the temperature profiles.

away from the wall as Pn_x is increased from zero. The slow down of the buoyancy-induced velocity near the wall decreases the heat transfer rate, and consequently increases the temperature near the heating surface. This is shown in Fig. 10 for the case of $\lambda = 0.5$.

The surface heat flux can be computed according to

$$\bar{q} = -k\left(\frac{\partial \bar{T}}{\partial \bar{y}}\right)_{\bar{y}=0}. \tag{130}$$

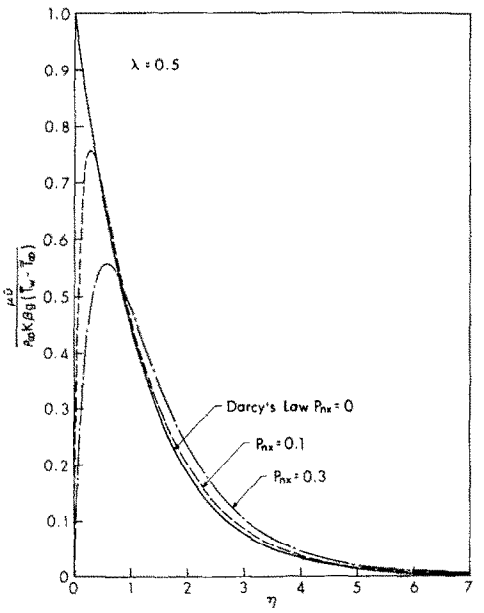

FIG. 9. Boundary effects on the velocity parallel to the heated plate.

Substituting equations (122a,b) into (130) yields

$$\frac{Nu_x}{\sqrt{Ra_x}} = \begin{cases} -g_0'(0) + 0(Pn_x \log Pn_x), & \lambda = 0 \quad (131a) \\ -g_0'(0) - Pn_x[\lambda - g_1'(0)] + 0(Pn_x^2), & \lambda > 0 \quad (131b) \end{cases}$$

where Nu_x is the local Nusselt number defined as $Nu_x = \bar{q}\bar{x}/k(\bar{T}_w - \bar{T}_\infty)$. Equation (131) for selected values of λ are presented in Fig. 11, where it is seen that the surface heat flux for $\lambda > 0$ decreases as Pn_x is increased. To see the effect of the local Darcy number on heat transfer rate, equation (131b) is rewritten as

$$Nu_x = -g_0'(0)\sqrt{Ra_x} - [\lambda - g_1'(0)]Ra_x\sqrt{Da_x} \tag{132a}$$

or

$$Nu_x = C_1(\lambda)\sqrt{Ra_x} - C_2(\lambda)Ra_x\sqrt{Da_x} \tag{132b}$$

when $C_1(\lambda) = -g_0'(0) = -g_0'(0)$ and $C_2(\lambda) = \lambda - g_1'(0)$. Equation (132) is plotted as Nu_x vs Ra_x in Fig. 12 at

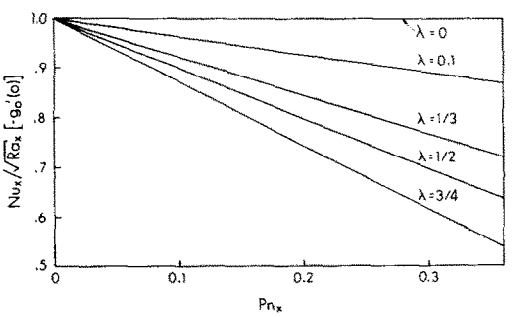

FIG. 11. Boundary effects on the local Nusselt number.

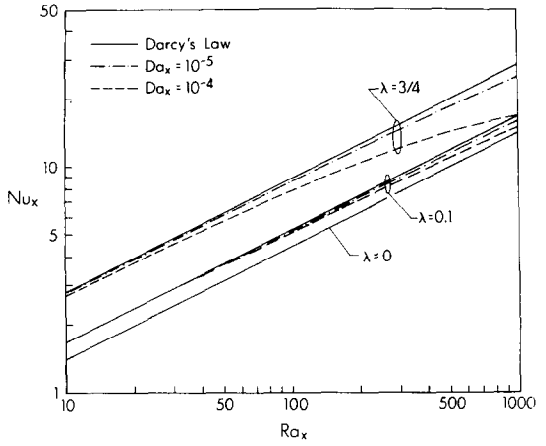

FIG. 12. Effects of the local Darcy number on the local Nusselt number.

constant values of Da_x for selected values of λ. It is seen that the value of the local Nusselt number decreases from that predicted based on Darcy's law as the value of Ra_x, Da_x or λ is increased.

The total thermal energy that is convected away at $\bar{x}$ is

$$\bar{Q} = \rho_\infty C \int_0^\infty \bar{u}(\bar{T} - \bar{T}_\infty)\,\mathrm{d}\bar{y}. \tag{133}$$

Substituting the leading term of equations (128a,b) and (129a,b) into equation (133) yields

$$\bar{Q} = k(\bar{T}_w - \bar{T}_\infty)Ra_x^{1/2}\left[-\frac{2g_0'(0)}{3\lambda+1} - \int_0^\infty g_0(\eta)\,\mathrm{e}^{-\eta/Pn_x}\,\mathrm{d}\eta\right] \tag{134}$$

where we have made use of equation (55b). For a vertical plate with a height l, the total heat transfer from the plate is equal to the total thermal energy that is convected away at $\bar{x} = l$. Thus, the total heat transfer rate for a vertical plate with a height l is given by equation (133) with $\bar{x} = l$, i.e.

$$\bar{Q} = k(\bar{T}_{w_l} - \bar{T}_\infty)Ra^{1/2}\left[-\frac{2g_0'(0)}{3\lambda+1} - \int_0^\infty g_0(\eta)\,\mathrm{e}^{-\eta/Pn}\,\mathrm{d}\eta\right] \tag{135}$$

where $P_n = \sqrt{Da\,Ra}$ with $Da = K/l^2$ and $Ra = \rho_\infty K\beta g A l^{\lambda+1}/\mu\alpha$. It is interesting to note that the integral in the last term of equation (135) represents the no-slip (or boundary) effect. The average Nusselt number as obtained from equation (135) is

$$\overline{Nu} = \frac{\bar{Q}}{k(\overline{T_w - T_\infty})}$$

$$= (1+\lambda)^{3/2}Ra^{1/2}\left[-\frac{2g_0'(0)}{3\lambda+1} - \int_0^\infty g_0(\eta)\,\mathrm{e}^{-\eta/Pn}\,\mathrm{d}\eta\right] \tag{136a}$$

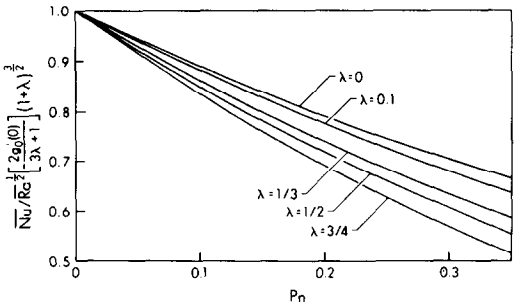

FIG. 13. Boundary effects on the average Nusselt number.

$$\frac{\overline{Nu}}{Ra^{1/2}\left[\dfrac{2(+\lambda)^{3/2}}{3\lambda+1}\right][-g_0'(0)]} = 1 - \frac{3\lambda+1}{2[-g_0'(0)]}\int_0^\infty g_0(\eta)\,\mathrm{e}^{-\eta/Pn}\,\mathrm{d}\eta \tag{136b}$$

where

$$\overline{(T_w - T_\infty)} = \frac{1}{l}\int_0^l (\bar{T}_w - \bar{T}_\infty)\,\mathrm{d}\bar{x} = \frac{Al^\lambda}{(\lambda+1)}.$$

Equation (136b) as a function of P_n for selected values of λ is plotted in Fig. 13, which shows that the average heat transfer rate decreases as the value of P_n is increased. The results presented in Fig. 13 are replotted in Fig. 14 for the average Nusselt number as a function of both Ra and Da. The solid straight lines in Fig. 14 represent the solutions based on Darcy's law [11]. It is shown that the higher the value of Da, the lower the value of Ra at which the value of Nu begins to deviate from that of the straight line.

7. CONCLUDING REMARKS

The following conclusions may be drawn from the present analysis:

(1) A new parameter Pn_x emerged from the present

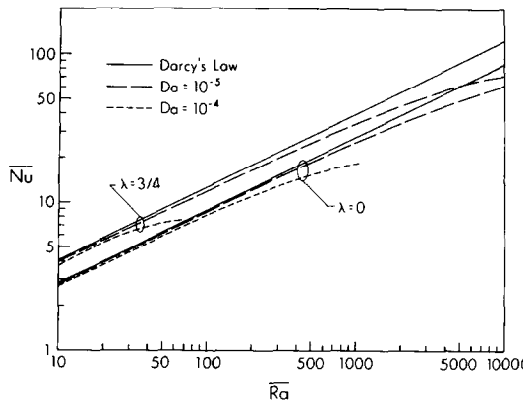

FIG. 14. Effects of the Darcy number on the average Nusselt number.

work for natural convection in a porous medium. The parameter Pn_x is defined as

$$Pn_x = (Ra_x Da_x)^{1/2} = (Gr_x Pr Da_x)^{1/2}$$
$$= K\sqrt{\frac{\rho_\infty g\beta(T_w - T_\infty)}{\phi\mu\alpha x}} = K\sqrt{\frac{\rho_\infty g\beta A x^{\lambda-1}}{\phi\mu\alpha}} \quad (137)$$

where $Gr_x = Kg\beta(T_w - T_\infty)x/\nu$ is the modified Grashof number in a porous medium. Physically, the value of Pn_x can be considered as the local thickness ratio of the viscous sublayer to that of the thermal layer, i.e.

$$Pn_x = \frac{\text{local viscous sublayer thickness}}{\text{local thermal layer thickness}}. \quad (138)$$

Thus, the formulation of natural convection heat transfer problems in a porous medium based on Darcy's law, where the viscous sublayer is neglected, corresponds to $Pn_x = 0$. Consequently, the results based on Darcy's law are accurate only if $Pn_x \ll 1$.

(2) The no-slip boundary conditions have a drastic effect on the streamwise (vertical) velocity component near the wall with a lesser effect on heat transfer characteristics. The viscous effect on the boundary slow down the buoyancy-induced flow near the wall. For $Pn_x = 0$, i.e. the Darcian flow, the maximum vertical velocity occurs at the wall resulting in a slip flow. As the value of Pn_x is increased from zero, the maximum vertical velocity decreases from the slip velocity. The distance from the wall, at which the maximum vertical velocity occurs, is increasing with the value of Pn_x.

(3) For $Pn_x \ll 1$, the local Nusselt number is found to be of the form

$$\frac{Nu_x}{(Ra_x)^{1/2}} = C_1(\lambda) - C_2(\lambda)Pn_x \quad (139a)$$

which can be rewritten as

$$Nu_x = C_1(\lambda)(Ra_x)^{1/2} - C_2(\lambda)Ra_x(Da_x)^{1/2} \quad (139b)$$

where $C_1(\lambda)$ and $C_2(\lambda)$ are positive constants with magnitude of the order of 0(1); their values depend on the wall parameter λ. For the case of isothermal plate ($\lambda = 0$), $C_2 = 0$ and equation (139) reduces to that given by Cheng and Minkowycz [11] which is based on Darcy's law.

(4) For $\lambda > 0$, theoretical results for the local surface heat flux based on Darcy's law formulation become inaccurate as the value of $Pn_x \gg 1$. It follows from equations (137a,b) that this occurs when either Ra_x or Da_x becomes very large. Since both Ra_x and Da_x depend on x, equations (137a,b) suggests that $Pn_x \gg 1$ occurs for large x if $\lambda > 1$ and for small x if $\lambda < 1$. The latter case corresponds to the location near the leading edge for an isothermal wall ($\lambda = 0$), which are in qualitative agreement with the numerical studies of Vafai and Tien [9] for forced convection porous layers and Evans and Plumb [10] for natural convection in porous layers.

(5) Although the first-order correction to the local Nusselt number is identically zero for an isothermal vertical flat plate (with $\lambda = 0$), its first-order correction to the average Nusselt number is negative, resulting in a decrease in the total heat transfer rate.

Acknowledgement —The authors gratefully acknowledge the support of the National Science Foundation on this work through grant No. MEA-8312095. They wish to thank T. Le for his assistance in the numerical computations.

REFERENCES

1. P. Cheng, Heat transfer in geothermal systems, *Advances in Heat Transfer*, **14**, p. 1. Academic Press (1978).
2. H. C. Brinkman, A calculation of the viscous force exerted by a flowing fluid on a dense swarm of particles, *Appl. Sci. Res.* **1**, 27–34 (1947).
3. B. K. C. Chan, C. M. Ivey and J. M. Barry, Natural convection in enclosed porous media with rectangular boundaries, *J. Heat Transfer* **92**, 21 (1970).
4. C. K. W. Tam, The drag on a cloud of spherical particles in low Reynolds number flow, *J. Fluid Mech.* **38**, 537 (1969).
5. T. S. Lundgren, Slow flow through stationary random beds and suspensions of spheres, *J. Fluid Mech.* **51**, 273 (1972).
6. Y. Katto and T. Masuoka, Criterion for the onset of convective flow in a fluid in a porous medium, *Int. J. Heat Mass Transfer* **10**, 297 (1967).
7. K. Walker and G. M. Homsy, A note on convective instability in Boussinesq fluids and porous media, *J. Heat Transfer* **99**, 338–339 (1977).
8. N. Rudraiah and T. Masuoka, Asymptotic analysis of natural convection through horizontal porous layer, *Int. J. Engng Sci.* **20**, 27–39 (1982).
9. K. Vafai and C. L. Tien, Boundary and inertia effects on flow and heat transfer in porous media, *Int. J. Heat Mass Transfer* **24**, 195–203 (1981).
10. G H. Evans and O. A. Plumb, Natural convection from a vertical isothermal surface imbedded in a saturated porous medium, *Proceedings of the AIAA–ASME Thermosphysics and Heat Transfer Conference*, Paper No. 78-HT-55 (1978).
11. P. Cheng and W. J. Minkowycz, Free convection about a vertical flat plate embedded in a porous medium with application to heat transfer from a dike, *J. geophys Res.* **82**, 2040–2044 (1977).
12. P. Cheng and C. T. Hsu, Higher-order approximations for Darcian free convective flow about a semi-infinite vertical flat plate, *J. Heat Transfer* **106**, 143 (1984).
13. K. Stewartson, On asymptotic expansions in the theory of boundary layers, *J. Math. Phys.* **36**, 173–191 (1957).

LE MODELE DE BRINKMAN POUR LA CONVECTION NATURELLE AU VOISINAGE D'UNE PLAQUE PLANE, VERTICALE, SEMI-INFINIE DANS UN MILIEU POREUX

Résumé—On utilise le modèle de Brinkman pour l'étude théorique des effets de frontière dans une convection naturelle en milieu poreux adjacent à une plaque verticale semi-infinie avec une variation de température selon $\tau_w \alpha \bar{x}$. On montre que les équations adimensionnelles du modèle contiennent deux paramètres $\varepsilon = (Ra)^{1/2}$ et $\sigma = (Da/\phi)^{1/2}$ où Ra et Da sont les nombres de Rayleigh et de Darcy basés sur une longueur de référence et ϕ la porosité. Pour la limite $\varepsilon \to 0, \sigma \to 0$ et $\sigma \ll \varepsilon$, une solution de perturbation est obtenue à partir de la méthode des développements asymptotiques. Le problème physique peut être visualisé en trois couches: une sous-couche visqueuse adjacente à la surface chaude, avec une épaisseur de l'ordre $0(\sigma)$; une couche thermique intermédiaire d'épaisseur d'ordre $0(\varepsilon)$; et une région d'écoulement potentiel d'épaisseur d'ordre 0(1). On trouve que le problème du premier ordre de la couche thermique est identique à celui basé sur la loi de Darcy avec écoulement de glissement, dont la solution a déjà été obtenue. Des solutions composites pour la fonction d'écoulement et la température, uniformément valables partout dans le champ d'écoulement, sont construitent à partir des solutions de la couche thermique et de la sous-couche visqueuse. Un nouveau paramètre $Pn_x = (Ra_x\, Da_x)^{1/2}$, avec Ra_x et Da_x étant les nombres de Rayleigh et de Darcy locaux rapportés à $\bar{x}$, est trouvé être une mesure de l'effet de frontière. On montre que l'effet visqueux sur la limite a un effet important sur la composante longitudinale de vitesse près de la paroi avec un moindre effet sur les caractéristiques de transfert de chaleur. En général, l'effet de frontière sur le nombre de Nusselt local devient plus prononcé quand les valeurs de Pn_x, Ra_x ou Da_x augmentent.

DAS BRINKMAN-MODELL FÜR NATÜRLICHE KONVEKTION AN EINER HALBUNENDLICHEN SENKRECHTEN PLATTE IN EINEM PORÖSEN MEDIUM

Zusammenfassung—Das Brinkman-Modell wurde angewandt für die theoretische Untersuchung von Begrenzungseinflüssen bei der natürlichen Konvektion in einer porösen Schicht, die an eine halbunendliche senkrechte Platte angrenzt. Die Wandtemperatur-Verteilung gehorcht dabei einer Potenzfunktion von der Form $\bar{T}_w \sim \bar{x}^{\lambda}$. Es wird gezeigt, daß die dimensionslosen Gleichungen für dieses Modell die beiden Parameter $\varepsilon = (Ra)^{1/2}$ und $\sigma = (Da/\phi)^{1/2}$ enthalten. Ra ist die Rayleigh-Zahl, Da die Darcy-Zahl und ϕ die Porosität. Es läßt sich veranschaulichen, daß das physikalische Problem aus drei Schichten aufgebaut ist: eine innere viskose Unterschicht an der Heizfläche mit einer Dicke von der Größenordnung $0(\sigma)$; eine mittlere thermische Schicht mit einer Dicke $0(\varepsilon)$; und das äußere Potentialströmungs-Gebiet mit einer Dicke 0(1). Ein neuer Parameter Pn_x—definiert als $Pn_x = (Ra_x\, Da_x)^{1/2}$, mit Ra_x und Da_x als der Rayleigh- bzw. Darcy-Zahl und $\bar{x}$ als Bezugslänge—stellt ein Maß für den Begrenzungseffekt dar. Der Reibungseffekt an der Begrenzung hat drastische Auswirkungen auf die Geschwindigkeitskomponente in Strömungsrichtung in Wandnähe, jedoch geringere Einflüsse auf den Wäremübergang. Der Begrenzungseffekt vermindert die Auftriebsströmung und damit auch den Wäremübergang. Die örtliche Nusselt-Zahl hat die Form $Nu_x/(Ra_x)^{1/2} = C_1 - C_2\, Pn_x$, wobei C_1 und C_2 von λ abhängen. Ganz allgemein wird der Einfluß der Begrenzung auf die örtliche Nusselt-Zahl für zunehmende Werte von Pn_x, Ra_x und Da_x stärker.

МОДЕЛЬ БРИНКМАНА ДЛЯ ЕСТЕСТВЕННОЙ КОНВЕКЦИИ У ПОЛУОГРАНИЧЕННОЙ ВЕРТИКАЛЬНОЙ ПЛОСКОЙ ПЛАСТИНЫ, ПОМЕЩЕННОЙ В ПОРИСТУЮ СРЕДУ

Аннотация—Для теоретического изучения граничных эффектов при естественной конвекции в пористом слое, прилегающем к полуограниченной вертикальной пластине с изменяющейся по степенному закону температурой стенки ($\bar{T}_w \alpha x^{-\lambda}$) применяется модель Бринкмана. Показано, что безразмерные определяющие уравнения, основанные на этой модели, содержат два параметра $\varepsilon = (Ra)^{1/2}$ и $\sigma = (Da/\phi)^{1/2}$, где Ra и Da—числа Рэлея и Дарси, основанные на относительной длине, ϕ—пористость. Для $\varepsilon \to 0$, $\sigma \to 0$ и $\sigma \ll \varepsilon$ получено решение задачи методом возмущений, при использовании метода сращиваемых асимптотических разложений. С физической точки зрения задача состоит из трех слоев: внутренний вязкий подслой, прилегающий к нагреваемой поверхности, с толщиной порядка $0(\sigma)$; средний тепловой слой, толщина которого $0(\varepsilon)$; и область внешнего потенциального течения с толщиной 0(1). Найдено, что краевая задача первого рода для теплового слоя идентична задаче, основанной на законе Дарси с проскальзывающим потоком, решение которой получено ранее. Из решений для теплового слоя и вязкого подслоя получены составные решения для функции тока и температуры, одинаково справедливые по всему полю течения. Новый параметр Pn_x, определяемый как $Pn_x = (Ra_x\, Da_x)^{1/2}$, где Ra_x и Da_x означают локальные числа Рэлея и Дарси, основанные на $\bar{x}$, является мерой граничного эффекта. Показано, что вязкостный эффект на границе оказывает резкое влияние на компоненту скорости, направленную по течению, вблизи стенки и меньше влияет на характеристики теплообмена. Граница затормаживает течение, вызванное подъемной силой, и в результате уменьшается теплообмен. Найдено, что местное число Нуссельта определяется соотношением $Nu_x/(Ra_x)^{1/2} = C_1 - C_2\, Pn_x$, где значения C_1 и C_2 зависят от λ. Для изотермической вертикальной пластины ($\lambda = 0$) поправка первого порядка к местному числу Нуссельта равна нулю, т.е. $C_2 = 0$. Влияние границы на местное число Нуссельта становится более выраженным с ростом Pn_x, Ra_x, Da_x.